

Received: 06 April 2023 / Accepted: 27 May 2023 / Published online: 30 May 2023

*vibratory peening, almen intensity,  
DOE method*

Maxime PAQUES<sup>1</sup>, Hong Yan MIAO<sup>1</sup>, Benoit CHANGEUX<sup>2</sup>,  
Sylvain TURENNE<sup>1</sup>, Jawad BADREDDINE<sup>2</sup>, Etienne MARTIN<sup>1\*</sup>

## **INVESTIGATION ON THE EFFECT OF THE VIBRATORY PEENING PROCESS PARAMETERS ON ALMEN INTENSITY**

Vibratory peening is a mechanical surface treatment process to improve both the fatigue life and smooth surface finish of metallic components in a single operation. Almen intensity is a significant parameter to relate the compressive residual stresses induced by the peening processes. In this study, the design of experiments (DOE) was used to investigate the effect of seven vibratory peening process parameters on Almen intensity. A specific vibratory peening machine, with the tub vibrating in a vertical pattern and resting on airbags, was built. Two empirical linear models were fitted. First, a screening model with primary effects showed that the media mass, airbag pressure, specimen longitudinal position, and lubrication rate have minor influence on Almen intensity. Secondly, a definitive model showed that high eccentricity, high frequency, and deep specimen immersion are required to reach high Almen intensities. The complex interactions between eccentricity, immersion depth, and frequency are described.

### **1. INTRODUCTION**

Vibratory peening is an emerging mechanical surface treatment process. It aims to combine fatigue life enhancement from shot peening and smooth surface finish from vibratory finishing within a single operation [1]. In shot peening, the component is exposed to a stream of shot to plastically deform its surface layers. This produces residual stresses which delay the surface crack propagation and therefore enhances the fatigue life of the treated component [2]. However, surface roughness increases due to the high energy impacts of small shot. It has a detrimental effect on the fatigue life due to surface crack initiation [3]. For this reason, vibratory finishing is used in addition to shot peening to reduce the surface roughness. In vibratory finishing, the component is freely dived in a U-shaped or bowl type tub filled with abrasive media, vibrating in a circular pattern [4]. The interaction between the vibrating media and the component produces surface polishing, which delivers smooth surface finish. The main concept of vibratory peening is similar to vibratory finishing, but the component is mechanically bound to the tub [1]. This increases the energy impacts between the media and the component. The vibratory peening eventually delivers surface plastic deformation and

---

<sup>1</sup> Génie Mécanique, Polytechnique Montréal, Canada

<sup>2</sup> Département de Matériaux & Procédés, Safran Tech, France

\* E-mail: [etienne.martin@polymtl.ca](mailto:etienne.martin@polymtl.ca)

<https://doi.org/10.36897/jme/166550>

residual stresses for fatigue life improvement but with similar surface roughness to those obtained by vibratory finishing [1, 5].

Most vibratory peening machines used in the literature are modified vibratory finishing machines. Generally, a specimen fixture is added to clamp the treated component in the tub. Recently, Canals et al. [6] performed the vibratory peening process with a vibratory peening machine where the tub has a flat bottom and vibrates in a vertical pattern. Compared to modified vibratory finishing machines where a U-shaped tub vibrates in circular motion, this flat bottom design with vertical vibration increases the impact energy between the media and the treated component. Besides, some studies used light abrasive media like those used in vibratory finishing [1, 5, 6]. Some others used steel media [7–11].

Almen intensity is an important parameter in the control of the shot peening process [12]. The main principle consists in treating thin standard Almen strips and measuring their deflection after different exposure times. The strip arc height increases with the exposure time until its saturation, which depends on the process parameters. Almen intensity is defined by the saturation value of the arc height. This parameter is used in industry to ensure the effectiveness and repeatability of the process [13]. Almen intensity is also used in the scientific literature as it relates the kinetic energy transferred from the shot stream to the treated component [12]. In shot peening, increasing Almen intensity generally produces more compressive and deeper residual stresses, eventually leading to higher fatigue life improvements. As a counterpart, the surface roughness usually increases with Almen intensity. Different ranges of Almen intensities are defined by the thickness of the strips. N strips are the thinnest and are used for the lowest intensity ranges, C strips are for the highest range, and A strips are the intermediate. Almen A are the most commonly used in shot peening and its applicability range is from 0.1 to 0.3 mmA [14].

Very few studies investigated the variation of Almen intensity for different vibratory peening process parameters. Canals et al. [6] performed vibratory peening using a mix of 3.18 to 6.35 mm diameter steel media in a tub vibrating in a vertical pattern. Different sets of media mass (555 and 792 kg) and frequency (from 23 to 47 Hz) were tested. They reported Almen intensity values ranging between 0.12 to 0.25 mmA. To the best of the authors knowledge, this is the highest Almen intensity observed in the literature of vibratory peening and was achieved for 792 kg of media and a frequency of 30 Hz. Unfortunately, the evaluation of each parameter effect is incomplete since the specimen immersion depth was not reported and not all levels of frequencies were tested for both media masses. Chan et al. [8] studied the combined effects of eccentricity between 40 and 75%, frequency between 20 and 25 Hz, and specimen immersion depth from 0 to 20 cm with a tub vibrating in a circular pattern. The highest Almen intensity they found was 0.11 mmN for 75% eccentricity, 20 Hz frequency, and 13 cm immersion depth. The effect of each parameter was not distinguished. Besides, no test was performed at 100% eccentricity and maximal frequency (25 Hz). Sangid et al. [7] compared the arc heights of Almen strips for different eccentricities at different processing times and for 16 Hz. The results showed that higher eccentricities produce higher arc heights. However, the Almen strip thickness was unknown, the Almen intensity value was not computed, and the eccentricity levels were not given. Kumar et al. [10, 15] reported an Almen intensity value of 0.1–0.13 mmA but only one set of vibratory peening process parameters was performed.

In the previous studies, different vibratory peening machines were used and none of these studies evaluated all the parameters under the same conditions. For example, the adjustable parameters, tub design, and tub vibration pattern were different for each machine. Therefore, the relative importance between the process parameters could not be evaluated, the critical parameters could not be identified and the interaction effects between the process parameters could not be estimated with the current state of the art. Besides, no statistical tools have ever been used to weigh the importance of the process parameters. To better understand the significance of the vibratory peening process parameters on Almen intensity, a large set of parameters from the same machine must be investigated using a statistical approach.

This study evaluates the influence of seven vibratory peening parameters on Almen intensity using the DOE methodology. A vibratory peening machine with adjustable parameters was developed for this study. A tub with a flat bottom vibrating in a vertical pattern was filled with 3 mm diameter steel media to maximize the media impacts on the treated components. The statistical tools from the DOE methodology such as empirical model fitting and ANOVA analysis were used to plan and analyse the experiments. Additional experiments were performed to validate the empirical model developed with the DOE method. The standard Almen intensity procedure was used to compute Almen intensity for 27 vibratory peening conditions from the seven vibratory peening process parameters.

## 2. EXPERIMENTAL METHODS

### 2.1. MACHINE DESIGN AND PROCESS PARAMETERS

The vibratory peening machine used for this study was built by Vibra Finish Ltd. and its schematic representation is shown in Fig. 1. The tub with flat bottom rests on airbags and is filled with media consisting of spherical ball bearings. AISI type 1015 carbon steel balls with 3 mm diameter and minimal hardness of 60 HRC are used. An electrical DC motor powers the in-phase rotation of two shafts in opposite directions at each side of the tub. This mainly produces a vibration of the tub in a vertical pattern.

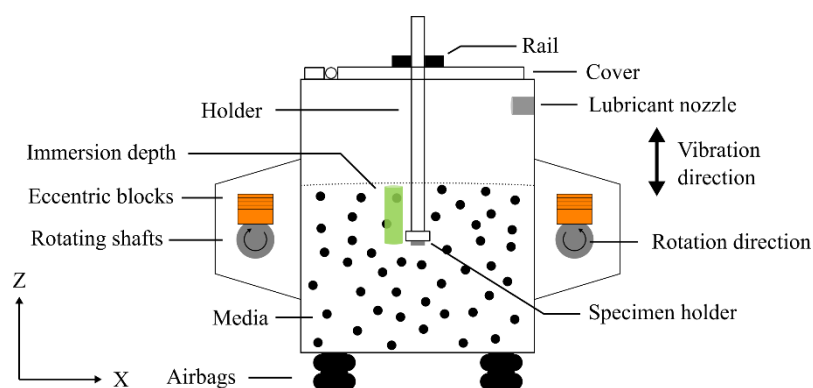


Fig. 1. Schematic representation of the vibratory peening machine showing a specimen clamped on the holder

The treated specimen is clamped onto a holder at a given immersion depth (see green column in Fig. 1) and the holder is unified with the cover through the rail. A constant flow of lubricant runs through the media to facilitate the media movement, drain particles, and regulate heat. The specimen surface is exposed to media impacts during the treatment, which is due to the relative movement between the fixed specimen and the free media. Surface plastic deformation is produced from the media impacts which aims to induce compressive residual stresses for fatigue life enhancement.

Seven process parameters were used to control this specific vibratory peening machine. The eccentric weight on the rotating shafts (X1\_Ecc) is adjusted by the mass of piled up and tightened eccentric blocks on the shafts. It is defined in kg/shaft and can be adjusted up to 24 kg/shaft. The media mass inside the tub (X2\_Mass) is adjusted manually by adding or removing media. The rotational frequency of the eccentric shafts (X3\_Freq) is adjusted up to 30 Hz with the DC motor drive command. The airbags pressure (X4\_Press) is adjusted up to 2.8 bars using manometers. The specimen immersion depth (X5\_Depth) is adjusted by inserting the specimen holder up and down into the tub through the cover. The part longitudinal position along the  $Y$  axis (X6\_Pos) is selected by using one of the three rails on the cover. The lubricant flow rate (X7\_Lub) is adjusted by the rotational speed of the lubricant pump, which is defined in rpm. In this article, a vibratory peening condition refers to a combination of these seven process parameters.

## 2.2. ALMEN INTENSITY MEASUREMENTS METHOD

In this study, the Almen intensity procedure defined for conventional shot peening described in SAE J442, J443 and J2597 [14, 16, 17] is applied to define the vibratory peening. Certified Almen N and A strips of  $76 \times 19$  mm<sup>2</sup> dimensions, having grade 1S were supplied by Electronics Inc. Almen A strips are 1.3 mm thick and Almen N strips are 0.8 mm thick [16]. For each test, an Almen strip was fixed on the holder and inserted inside the media at the given X5\_Depth after adjustment of the six other parameters. The processing time was determined by the machine running time. After the treatment, the Almen strip was removed from the media and unclamped. The Almen strip bends due to the surface plastic deformation and its arc height was measured using EI TSP-3 Almen gage. For each vibratory peening condition, at least four treatments were performed at different processing times. Saturation curves were constructed by fitting the measured arc heights and the processing time using the following equation from J2597 [17]:

$$h(t) = a \left( 1 - e^{-\frac{b}{t}} \right) \quad (1)$$

where  $t$  is the vibratory peening processing time,  $h(t)$  is the arc height and  $a$ ,  $b$  are the model parameters which were fitted using the least square method. A routine coded with Python was used for the fitting of Equation (1) on the measured arc heights. This routine was verified accordingly to [17]. Almen intensity was defined as the arc height at which doubling  $t$  increased  $h(t)$  by 10% [14].

For most of the tests in this study, the saturation curves were performed using Almen N strips. However, Almen A was used for the Almen intensities that produced arc heights above

0.1 mmA, as recommended in J443 [14]. Since the results must be expressed in the same scale for the DOE analysis, the Almen A-type intensities were converted into Almen N-type intensities according to the following procedure. First, an Almen arc height conversion equation was established experimentally. The results are shown in Fig. 2.

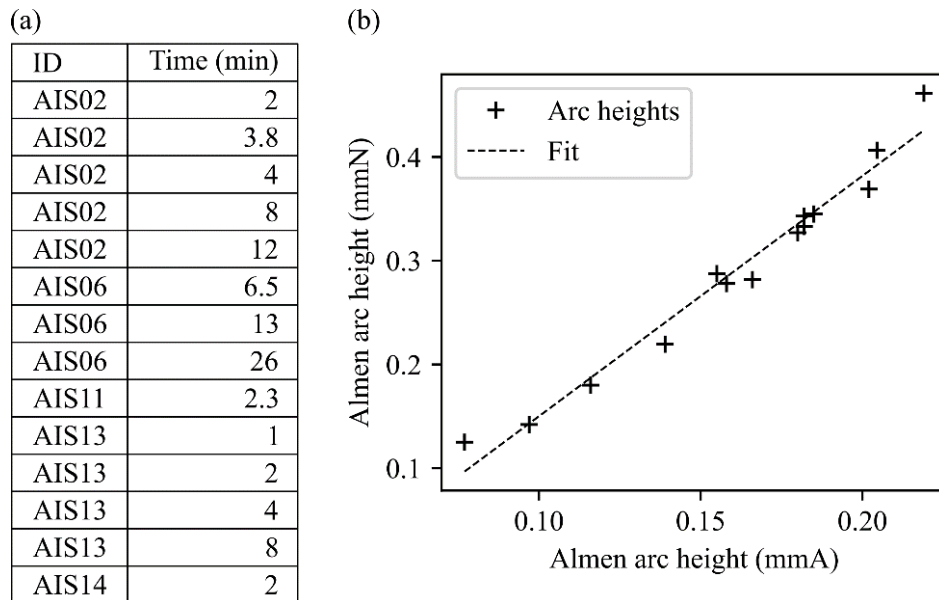


Fig. 2. Almen N arc height as a function of Almen A arc heights produced by vibratory peening. In (a), the vibratory peening conditions are from Table 1 in Section 2.4. In (b), the conversion between Almen N strip and Almen A strip was deduced from the fitted equation

Almen N and A strips were treated for the same vibratory peening conditions, which are given in Fig. 2a. Fig. 2b presents the Almen N strips arc heights as a function of Almen A arc heights. The linearity of the experimental results allowed to determine the following arc height conversion equation:

$$N \text{ arc height} = 2.32 \times A \text{ arc height} - 0.08. \quad (2)$$

Second, the Equation (2) was used to convert the Almen arc heights from A-type into N-type arc heights. Finally, the N-type Almen intensities was obtained by reproducing the saturation curves using the converted A-type Almen arc heights.

### 2.3. SELECTION OF THE VIBRATORY PEENING PARAMETER RANGES FOR THE DOE

The DOE method was used to study the effect of the seven vibratory peening parameters on Almen intensity using a factorial approach. A fractional screening design with factors varying at two levels was selected. The factors' levels are selected to test the largest ranges of the vibratory peening parameters. Figure 3 summarizes the levels for the seven investigated process parameters in this DOE. The minimal and maximal levels for each factor are given in Fig. 3a and their selection are detailed in this section. Some are given by the machine set-up and limitations; some others are set to achieve sufficient Almen strip arc heights.

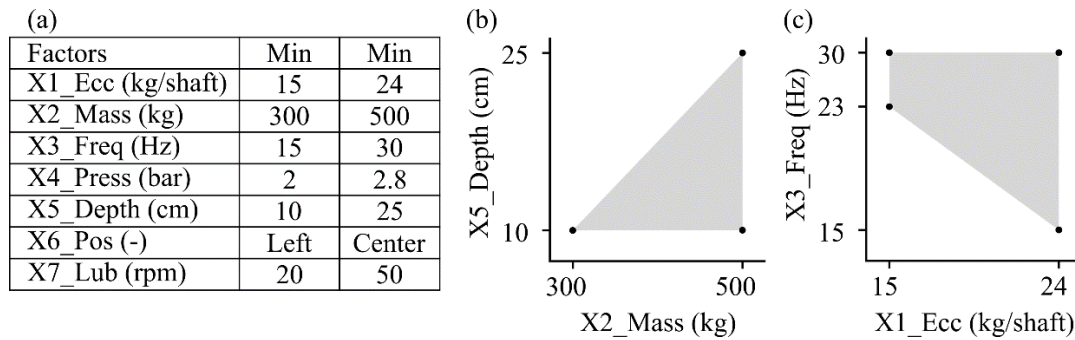


Fig. 3. Design of experiment method showing (a) the upper and lower levels of the seven process parameters and the restricted level variation range of (b) X5\_Depth as a function of X2\_Mass, and (c) X3\_Freq as a function of X1\_Ecc

The minimal and maximal levels for X4\_Press, X6\_Pos and X7\_Lub are set by the machine limitations. The minimal X4\_Press is 2 bars to avoid collisions between the tub and the structure of the machine. Among the three possible positions for X6\_Pos, only the left and center positions were considered because it was assumed that the left and right positions are equivalent due to the symmetry of the tub. The minimal X7\_Lub of 20 rpm was set to avoid rusting of the media and the maximum of 50 rpm was set to avoid accumulating lubricant inside the tub.

X2\_Mass and X5\_Depth are two dependent process parameters because the total height of media in the tub depends on X2\_Mass and their variation is summarized in Fig. 3b. The range of X5\_Depth inevitably decreases with X2\_Mass as described by the following inequation:

$$x2_{Mass} - x5_{Depth} \geq 0, \tag{3}$$

where  $x2_{Mass}$ , and  $x5_{Depth}$  are the levels on a coded scale from -1 to +1 of X2\_Mass and X5\_Depth, respectively. A minimum value of X5\_Depth = 10 cm was selected to ensure a steady media movement around the specimen. This required a minimal media height of 20 cm in the tub, which corresponds to the minimum value of X2\_Mass = 300 kg. The maximal media height in the tub was 35 cm, which corresponds to the maximum value of X2\_Mass = 500 kg. To allow 10 cm media above the specimen, the maximal value of X5\_Depth is 25 cm when X2\_Mass = 500 kg.

The dependence between X1\_Ecc and X3\_Freq is summarized in Fig. 3c. The maximal levels were set by the machine limitations (X1\_Ecc = 24 kg/shaft, X3\_Freq = 30 Hz). The minimal levels for these two process parameters were determined to ensure sufficient plastic deformation for processing time of 20 min. A minimal Almen strip arc height of 0.08 mmN was verified for every vibratory peening condition. The effect of X1\_Ecc and X3\_Freq on Almen strip arc heights were evaluated. Almen N strips were used since they relate lower ranges of intensities. Figure 4 plots the arc heights for different levels of X1\_Ecc as a function of X3\_Freq. The X1\_Ecc is given in the top left corner of each subplot, with the minimal level 15 kg/shaft on the left (see Fig. 4a) and the maximal level 24 kg/shaft on the right (see Fig. 4b). The other parameters X2\_Mass, X4\_Press, X5\_Depth, X6\_Pos and X7\_Lub were randomly selected for each test. The green areas represent the accepted variation ranges of the parameters.

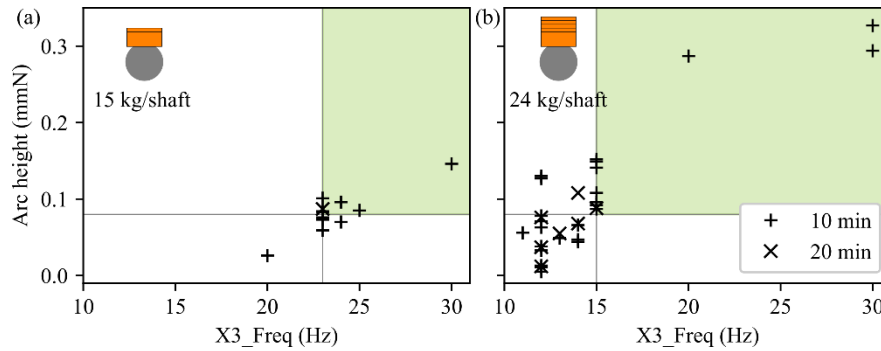


Fig. 4. The effect of X3\_Freq on arc heights of Almen N strips after vibratory peening for, (a) X1\_Ecc=15 kg/shaft and (b) X1\_Ecc=24 kg/shaft. For each test, X2\_Mass, X4\_Press, X5\_Depth and X7\_Lub were randomly varied. X6\_Pos was fixed at the centre

For any level of the five other vibratory peening parameters, the Almen arc heights are above 0.08 mmN in these accepted ranges. X1\_Ecc = 15 kg/shaft allows a minimal level of 23 Hz for X3\_Freq, as shown in Fig. 4a. For X1\_Ecc = 24 kg/shaft, the lower level of X3\_Freq is 15 Hz in Fig. 4b. The levels variation of the two factors is limited by the following linear relationship:

$$0.53 \times x1_{Ecc} + x3_{Freq} \geq -0.47, \quad (4)$$

where  $x1_{Ecc}$ , and  $x3_{Freq}$  are the level on a coded scale from  $-1$  to  $+1$  of X1\_Ecc and X3\_Freq, respectively.

#### 2.4. DESIGN OF EXPERIMENTS

The DOE method was used to create the tests matrix, fit the empirical models, and perform the statistical analysis. A non-standard screening factorial design was selected to relate the effects of the seven vibratory peening parameters on Almen intensity. Equations (3) and (4) were considered to relate the factors constraints in Fig. 3b and 3c. Two repetitions were considered for each vibratory peening condition to create the tests matrix. Table 1 shows the resulting tests matrix with 16 tests to estimate the effects of the seven process parameters as primary factors on Almen intensity.

Table 1. Non-standard fractional screening tests matrix with two replications used to build the two empirical models

ID	X1_Ecc (kg/shaft)	X2_Mass (kg)	X3_Freq (Hz)	X4_Press (bars)	X5_Depth (cm)	X6_Pos (-)	X7_Lub (rpm)
AIS01	24	500	15	2	25	Center	50
AIS02	24	500	30	2.8	10	Left	50
AIS03	15	500	30	2.8	10	Center	50
AIS04	15	500	23	2	25	Left	50
AIS05	15	500	30	2.8	25	Left	20
AIS06	15	300	30	2.8	10	Center	20
AIS07	15	300	30	2	10	Center	50
AIS08	24	500	15	2	10	Left	20

AIS09	24	300	15	2.8	10	Center	20
AIS10	24	300	30	2	10	Left	50
AIS11	24	500	30	2.8	25	Left	50
AIS12	24	300	30	2	10	Left	20
AIS13	24	500	30	2	25	Center	20
AIS14	24	500	30	2.8	25	Center	20
AIS15	15	500	30	2	10	Left	20
AIS16	24	500	15	2	10	Center	20

The run order of the tests was randomized for ensuring the observations to be independently distributed random variables [18]. In this study, a confidence interval of 99% was used. This implies P-value threshold of 0.01 to indicate the statistical significance of the variables on the response [18].

Two empirical linear models were fitted on the resulting Almen intensities. First, a screening model with all the seven parameters as primary factors was fitted to identify three major process parameters on Almen intensity. Secondly, a definitive model using only the three major parameters as primary and two-factors interactions was fitted to describe the variation of Almen intensity.

## 2.5. MODEL VALIDATION EXPERIMENTS

Additional experiments were performed to validate the model developed using the DOE method. Intermediate levels of X3\_Freq (17.5-30 Hz) were tested for two levels of X5\_Depth (25 and 28 cm). The X2\_Mass (500 and 544 kg) must be adjusted with respect to the X5\_Depth as explained in Section 2.3. The other vibratory peening parameters were kept constant. The vibratory peening conditions for the model validation are listed in Table 2. Each condition was repeated twice.

Table 2. Additional set of experiments performed for the empirical model validation

ID	X1_Ecc (kg/shaft)	X2_Mass (kg)	X3_Freq (Hz)	X4_Press (bars)	X5_Depth (cm)	X6_Pos (-)	X7_Lub (rpm)
MV01	24	500	20	2.8	25	Center	20
MV02	24	500	22.5	2.8	25	Center	20
MV03	24	500	25	2.8	25	Center	20
MV04	24	500	27.5	2.8	25	Center	20
MV05	24	500	30	2.8	25	Center	20
MV06	24	544	17.5	2.8	28	Center	20
MV07	24	544	20	2.8	28	Center	20
MV08	24	544	22.5	2.8	28	Center	20
MV09	24	544	25	2.8	28	Center	20
MV10	24	544	27.5	2.8	28	Center	20
MV11	24	544	30	2.8	28	Center	20

### 3. EXPERIMENTAL RESULTS

#### 3.1. ALMEN INTENSITIES OBTAINED FOR THE DOE

Table 3 lists the 32 experimental results obtained with the DOE. The Almen intensity value at each repetition is given for each of the 16 vibratory peening conditions from Table 1. The results are ranging from 0.084 mmN to 0.396 mmN. The Almen intensities for tests 21, 22, 25, 26, 27 and 28 were obtained first using Almen A-strips, and then converted to Almen N intensities following the procedure described in Section 2.2.

The repeatability of the process was evaluated using the dispersion in Almen intensity observed in the results of the DOE. All the Almen intensities listed in Table 3 are shown in Fig. 5 and are compared with the dispersion for each vibratory peening condition. The dispersion is obtained by subtracting the two repetitions tests for each condition. The highest dispersion is 0.038 mmN and was obtained for the AIS016 condition. This represents only half of the tolerance range of 0.075 mm defined in AMS2430T [19] confirming the acceptable repeatability of the vibratory peening process for industrial applications.

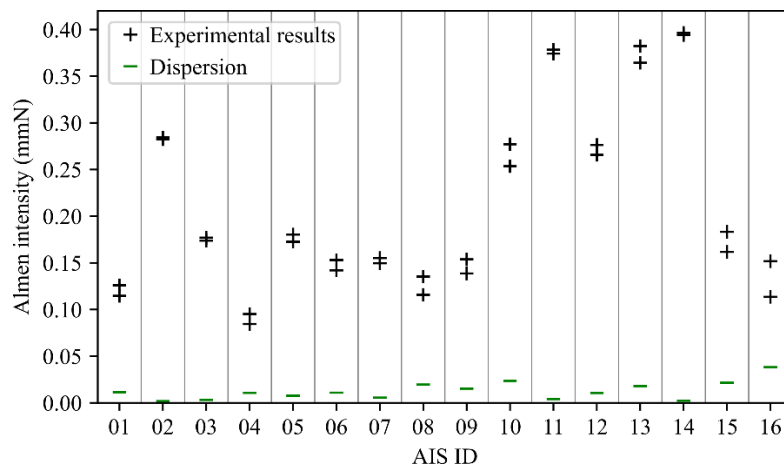


Fig. 5. Measured Almen intensities for 32 vibratory peening conditions from the test matrix with the associated dispersion between the repetitions. Dispersion is computed as the difference between the maximal and minimal intensities measured for each condition

#### 3.2. IDENTIFICATION OF THE MAJOR VIBRATORY PEENING PARAMETERS USING A SCREENING MODEL

The least squares method has been used to fit a linear empirical model and identify the major vibratory peening parameters. The following screening model was obtained using the effect of the seven primary factors on the Almen intensity data from Table 3:

$$\begin{aligned}
 y = & 1.49 \times 10^{-1} + 7.77 \times 10^{-2} x_{1_{Ecc}} + 1.25 \times 10^{-2} x_{2_{Mass}} + 9.87 \times 10^{-2} x_{3_{Freq}} \\
 & + 7.88 \times 10^{-3} x_{4_{Press}} + 1.79 \times 10^{-2} x_{5_{Depth}} - 1.05 \times 10^{-2} x_{6_{Pos}} \\
 & - 9.41 \times 10^{-3} x_{7_{Lub}} + \varepsilon
 \end{aligned} \quad (5)$$

where  $y$  is the Almen intensity predicted by the model and  $x$  are the level on a coded scale from  $-1$  to  $+1$  of the factors associated to the vibratory peening process parameters.

Table 3. Design matrix and the resulting Almen intensities obtained with process conditions described in Table 1

Test	ID	REP	Almen intensity	
			(mmN)	(mmA)
01	AIS01	1	0.115	-
02	AIS01	2	0.126	-
03	AIS02	1	0.282	-
04	AIS02	2	0.284	-
05	AIS03	1	0.174	-
06	AIS03	2	0.177	-
07	AIS04	1	0.095	-
08	AIS04	2	0.084	-
09	AIS05	1	0.180	-
10	AIS05	2	0.173	-
11	AIS06	1	0.142	-
12	AIS06	2	0.153	-
13	AIS07	1	0.155	-
14	AIS07	2	0.150	-
15	AIS08	1	0.116	-
16	AIS08	2	0.135	-
17	AIS09	1	0.154	-
18	AIS09	2	0.139	-
19	AIS10	1	0.254	-
20	AIS10	2	0.277	-
21	AIS11	1	0.378	0.190
22	AIS11	2	0.374	0.190
23	AIS12	1	0.276	-
24	AIS12	2	0.266	-
25	AIS13	1	0.382	0.195
26	AIS13	2	0.364	0.187
27	AIS14	1	0.396	0.195
28	AIS14	2	0.394	0.195
29	AIS15	1	0.162	-
30	AIS15	2	0.183	-
31	AIS16	1	0.114	-
32	AIS16	2	0.152	-

The Pareto chart of effects in Fig. 6 were used to determine the importance of the vibratory peening process parameters on Almen intensity. The F-values of the variables with their associated P-values [18] are given in Table 4.

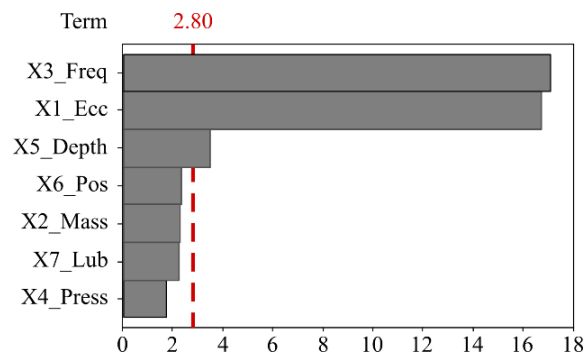


Fig. 6. Pareto chart of standardized effect of the primary factors on Almen intensity. Factors on the right of the reference line at 2.80 are statistically significant

The major parameters are X1\_Ecc, X3\_Freq and X5\_Depth with P-values falling below 0.01. This clearly indicates the influence of these factors on Almen intensity with a confidence interval above 99%. The Pareto chart of effect in Fig. 6 shows the absolute of the  $t$ -values of the effects given in Table 4. This graph allows to rank the effects importance of the vibratory peening parameters on Almen intensity from the largest to the smallest. The dotted reference line at 2.80 represents the threshold of statistical significance. This is the  $t$ -value for the 99% confidence interval of a  $t$ -distribution for a range of one-sided critical region and with 24 degrees of freedom. The latter is the number of degrees of freedom for the error term

(see Table 4). X1\_Ecc, X3\_Freq and X5\_Depth are the major vibratory peening parameters, which agrees with the conclusion of the ANOVA analysis. The X1\_Ecc and X3\_Freq appear to be much more important than the X5\_Depth. Conversely, the X2\_Mass, X4\_Press, X6\_Pos and X7\_Lub are the minor factors. For the considered data, their effect on the vibratory peening Almen intensity are about 10 times less important than X1\_Ecc and 7 times less than X3\_Freq, which is negligible.

Table 4. ANOVA for the screening model with primary effects on Almen intensity. Statistically significant variables are highlighted in grey. “DF” stands for degree of freedom, “Adj.” for adjusted, “SS” for sum of squares, “MS” for mean square, “Coef.” for the coefficient of the factor on the coded scale and “SE” for standard error

Source	DF	Adj SS	Adj MS	F-Value	P-Value	Coef.	SE Coef.	t-value
Model	7	0.292	0.042	78.10	0.000	0.150	0.007	22.650
X1_Ecc	1	0.150	0.150	281.27	0.000	0.077	0.005	16.770
X2_Mass	1	0.003	0.003	5.31	0.030	0.013	0.005	2.300
X3_Freq	1	0.157	0.157	293.53	0.000	0.099	0.006	17.130
X4_Press	1	0.002	0.002	3.08	0.092	0.008	0.004	1.750
X5_Depth	1	0.007	0.007	12.24	0.002	0.018	0.005	3.500
X6_Pos	1	0.003	0.003	5.37	0.029	0.010	0.005	2.320
X7_Lub	1	0.003	0.003	5.00	0.035	-0.009	0.004	-2.240
Error	24	0.013	0.001					
Lack-of-Fit	9	0.011	0.001	9.14	0.000			
Pure Error	15	0.002	0.000					
Total	31	0.304						
$R^2 = 95.8\%$								

The screening model regression adequacy was verified with the residues analysis in Fig. 7 and the ANOVA in Table 4. The normal probability plot is shown in Fig. 7a confirms the normal distribution of the residuals without outliers.

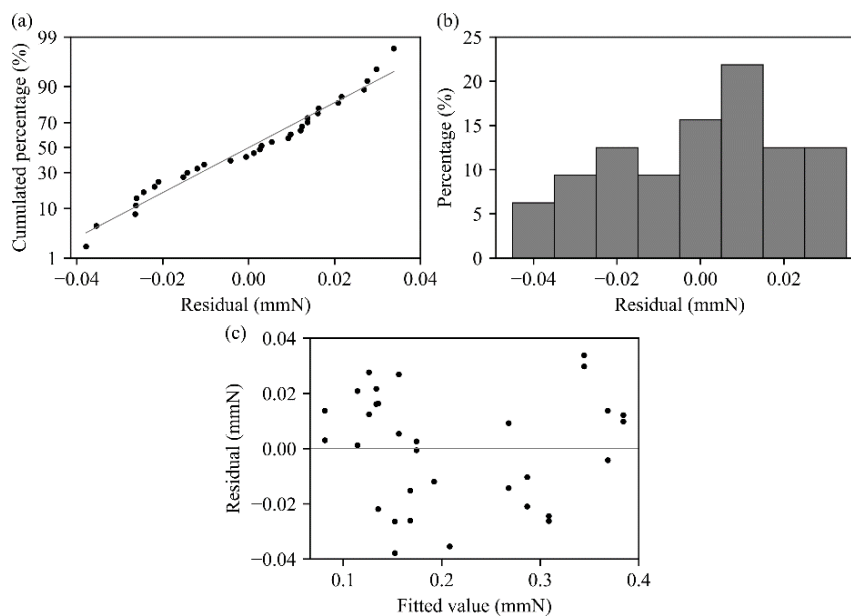


Fig. 7. Residues analysis of the screening model with primary effects on Almen intensity. (a) The aligned distribution of the residuals on the normal probability plot. (b) The histogram of the residuals centred at 0. (c) The residues as a function of the predicted values without specific pattern or general trend in the mean values

The histogram of the residuals in Fig. 7b shows that the residues are centred at zero. Fig. 7c plots the residuals as a function of the fitted value. No specific pattern is observed, which means that the model is not biased by the fitted value. The residues as a function of the run order are not plotted because the run order was randomized. Therefore, no biasing due to variable change are expected. Finally, the residues analysis validates the normality assumption. The ANOVA analysis in Table 4 shows that the regression model is statistically significant with a P-value below 0.01. Besides, the model fits the data with a  $R^2$  of 95.8%. However, the lack-of-fit value exhibits a P-value below 0.01, which indicates that the screening model from Equation (5) does not predict the Almen intensity adequately. This means that higher degree factors, like two-factor interactions or quadratic terms, are missing in the model. For this reason, this model is only used to identify the major vibratory peening parameters for establishing a definitive model.

### 3.3. DEFINITIVE MODEL DESCRIBING THE EFFECT OF THE MAJOR VIBRATORY PEENING PARAMETERS ON ALMEN INTENSITY

A new regression model was developed using only the three major vibratory peening parameters identified in Section 3.2 (X1\_Ecc, X3\_Freq and X5\_Depth). It now includes both primary and two-factor interaction effects to improve the lack of fit obtained in the screening model (Equation (5)). The definitive model is given by:

$$\begin{aligned}
 y = & 1.67 \times 10^{-1} - 6.02 \times 10^{-2}x_{1Ecc} - 8.11 \times 10^{-2}x_{3Freq} - 2.00 \times 10^{-5}x_{5Depth} \\
 & + 1.88 \times 10^{-2}x_{1Ecc}x_{3Freq} + 2.35 \times 10^{-2}x_{1Ecc}x_{5Depth} \\
 & + 3.07 \times 10^{-2}x_{3Freq}x_{5Depth} + \varepsilon
 \end{aligned}
 \tag{6}$$

The definitive model regression adequacy was verified with the residual analysis in Fig. 8 and ANOVA in Table 5.

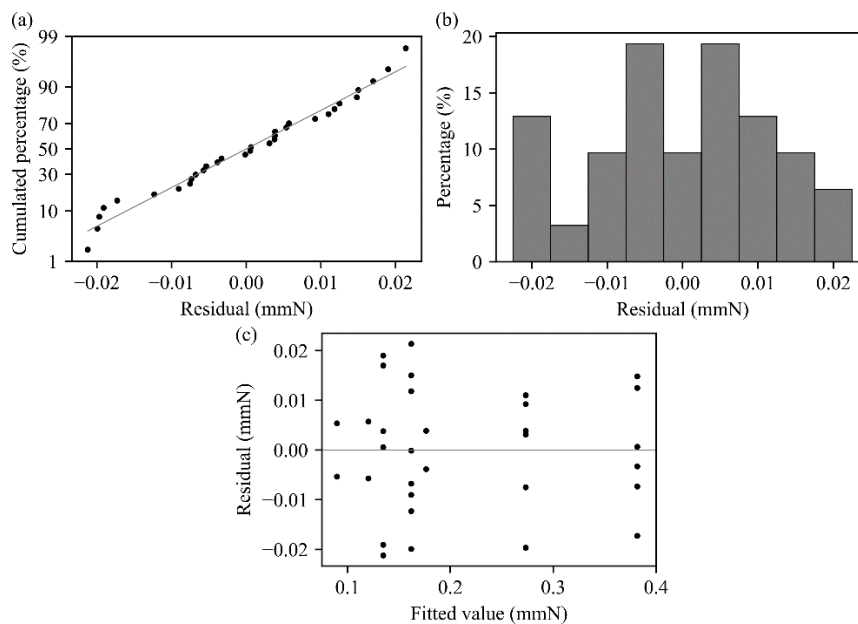


Fig. 8. Residues analysis for the definitive model between the vibratory peening factors and Almen intensity. (a) The aligned distribution of the residuals on the normal probability plot. (b) The histogram of the residuals centred at 0. (c) The residues as a function of the predicted values without specific pattern or general trend in the mean values

Table 5. ANOVA analysis for the definitive model between vibratory peening and Almen intensity

Source	DF	Adj SS	Adj MS	F-Value	P-Value	Coef.	SE Coef.	t-Value
Model	6	0.300	0.050	275.45	0	0.167	0.006	26.900
X1_Ecc	1	0.016	0.016	85.45	0	0.060	0.007	9.240
X3_Freq	1	0.021	0.021	117.55	0	0.081	0.007	10.840
X5_Depth	1	0.000	0.000	0.00	0.995	0.000	0.004	0.010
X1_Ecc*X3_Freq	1	0.001	0.001	5.97	0.022	0.019	0.008	2.440
X1_Ecc*X5_Depth	1	0.009	0.009	50.62	0	0.023	0.003	7.110
X3_Freq*X5_Depth	1	0.015	0.015	83.04	0	0.031	0.003	9.110
Error	25	0.005	0.000					
Lack-of-Fit	10	0.003	0.000	1.94	0.118			
Pure Error	15	0.002	0.000					
$R^2 = 98.5\%$								

Figure 8a shows that the residues follow a normal distribution without outliers. The residues are centred at zero in Fig. 8b and do not show a specific pattern in Fig. 8c. This validates the normality for residues. The ANOVA analysis in Table 5 shows that the model is statistically significant (p-value <0.01), fits the data with a  $R^2$  value of 98.5%, and does not exhibit a lack-of-fit (p-value <0.01). This means that the definitive model given by Equation (6) has a higher prediction accuracy than the screening model given by Equation (5). The primary effect of X5\_Depth is not statistically significant (p-value > 0.1) but is kept in the model. This is because the two-factor interaction effects of X5\_Depth with X1\_Ecc (X1\_Ecc\*X5\_Depth) and X3\_Freq (X3\_Freq\*X5\_Depth) are significant. The two-factor interaction effect between X1\_Ecc and X3\_Freq is not statistically significant (p-value > 0.01). However, it is kept in the equation as it improves the  $R^2$  and  $p$ -value for the lack-of-fit.

### 3.4. VALIDATION OF THE DEFINITIVE EMPIRICAL MODEL

The DOE model described in Eq. (6) must be converted in engineering units to allow comparing the predictions with the experimental data. The DOE model is fitted using coefficients for the factors  $X$  expressed in engineering units (such as given in Fig. 3). The resulting definitive model is:

$$\begin{aligned}
 y = & 3.61 \times 10^{-1} - 1.14 \times 10^{-2} \times X1_{Ecc} - 9.65 \times 10^{-3} \times X3_{Freq} - 2.58 \times 10^{-2} \times X5_{Depth} \\
 & + 5.59 \times 10^{-4} \times X1_{Ecc} \times X3_{Freq} + 6.95 \times 10^{-4} \times X1_{Ecc} \times X5_{Depth} \quad (7) \\
 & + 5.46 \times 10^{-4} X3_{Freq} \times X5_{Depth}.
 \end{aligned}$$

Comparisons between the additional validation data shown in Table 2 and the model predictions from Equation (7) are presented in Fig. 9. A X2\_Mass = 500 kg with the associated maximal X5\_Depth of 25 cm was used in Fig. 9a. A higher X2\_Mass of 544 kg was used in Fig. 9b to increase X5\_Depth up to 28 cm (see Section 2.3 and 2.4). The Almen intensities are expressed in A-type using the conversion method described in Section 2.2. The  $R^2$  value evaluates the accuracy of the predictions. In Fig. 9a, the  $R^2$  was computed without considering for the outlier. In Fig. 9a and 9b, the model can predict all the experimental Almen intensities generated here with more than 87.5% of accuracy. The Almen intensity increases linearly with the increase of X3\_Freq with the same slope for both

experimental results and model predictions. This confirms that a simple linear model can be used to describe the Almen intensity variation during vibratory peening for the conditions presented in this study.

In Fig. 9a, the experimental result for X3\_Freq = 25 Hz shows a lower Almen intensity than the model prediction. One possible explanation can be by a specific resonance mode of the tub leading to a different tub and media movement under this specific vibratory peening condition. This did not occur for a higher X2\_Mass because the mass of the tub was different, which changes the natural frequency of the tub. Further investigations are required on the tub movement as well as on the relationship between the tub and media movement to better understand this phenomenon.

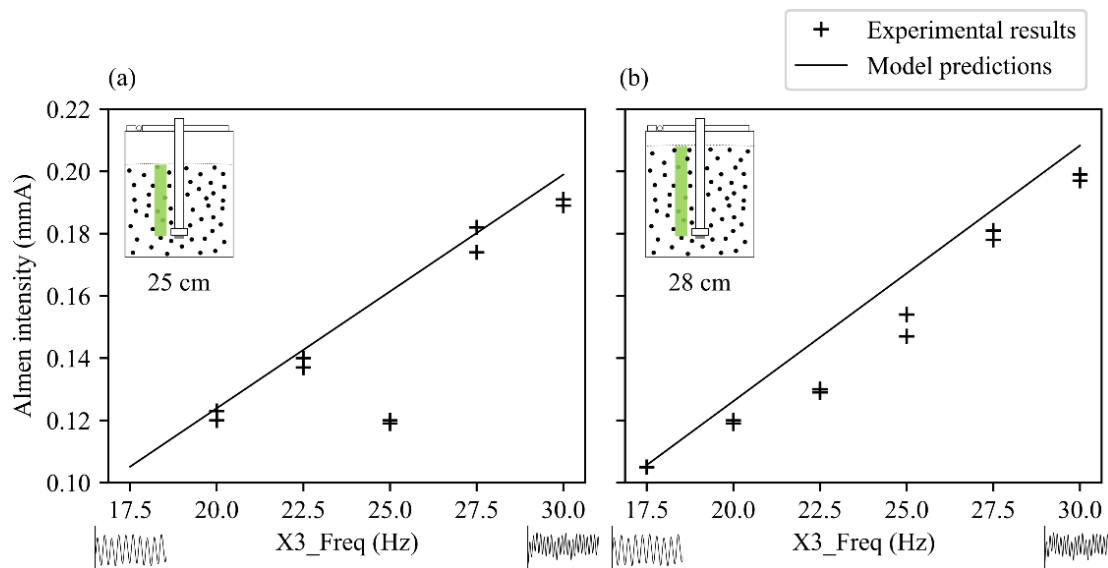


Fig. 9. Comparison between the linear model predictions from Equation (7) and validation Almen intensities data as a function of X3\_Freq. The other levels are shown in Table 2 and correspond to (a) MV01 to MV05 (X2\_Mass = 500 kg) and (b) MV06 to MV11 (X2\_Mass = 544 kg). The  $R^2$  value compares the experimental data and the DOE model predictions

## 4. DISCUSSION

### 4.1. MINOR VIBRATORY PEENING PARAMETERS ON ALMEN INTENSITY

The ANOVA analysis and Pareto chart of effects (see Table 4 and Fig. 6) for the screening model from Equation (5) showed that the airbags pressure, lubricant rate, media mass and longitudinal part position are minor vibratory peening parameters on Almen intensity. The airbags are used as dampers to isolate the vibrating tub from the ground. They have a negligible effect on the movement of the vibrating tub when compared with the rotating shaft, which is shown in Fig. 1. The lubricant is important to the vibratory peening process because it controls the friction between media during the process. Wang et al. [20] studied the effect of the lubricant on the media impact force. Three different lubricants were investigated, and the study showed that the friction coefficient significantly affects the media velocity. In this study, the lubricant flow rate has to be high enough to ensure that all the

media are covered. The flow rate must also remain below a critical value to avoid media overflow. However, between these two values, results shown in the Pareto chart in Fig. 6 suggests that the effect of lubricant flow rate has a negligible effect on the overall friction between the media.

Canals et al. [6] observed a significant effect of the media mass on Almen intensity. However, they did not differentiate the part immersion depth with the media mass. The part immersion depth automatically increases when more media is added to the tub to increase the media mass (see Section 2.3). In the present study, both parameters were considered independently, showing that the immersion depth is a major parameter to increase Almen intensity during vibratory peening, while the overall media mass present in the tub is negligible. This suggests that, on the one hand, the depth of the tub is critical to the vibratory peening process since it allows modifying the immersion depth. On the other hand, changing the tub length and width have a much smaller effect on the process since it only affects the media mass. This is supported by the negligible effect of part longitudinal position observed in this study. This may be because the bottom of the tub is flat and vibrates in a vertical motion leading to a similar media movement at any position for a given part immersion depth.

#### 4.2. MAJOR VIBRATORY PEENING PARAMETERS ON ALMEN INTENSITY

The Pareto chart of effects in Fig. 6 showed that the rotating shafts eccentricity and frequency are the two most important vibratory peening parameters on Almen intensity. This is because Almen intensity is related to the kinetic energy transmitted from the media to the treated surface [12]. Increasing the eccentric weights and the frequency increases the media kinetic energy generated by the rotating shafts [4]. This is shown in Fig. 10 where the Almen intensity evolution for these two parameters is presented. The Almen intensity are predicted using Equation (7) as a function of X1\_Ecc for the minimal and maximal levels of X3\_Freq and X5\_Depth on the left (see Fig. 10a) and as a function of X3\_Freq for the minimal levels of X1\_Ecc and X5\_Depth on the right (see Fig. 10b). The Almen intensity increases with the increase of eccentricity (Fig. 10a) and frequency (Fig. 10b) for all part insertion depths investigated here. This agrees well with previous works showing improvement in Almen intensity with these two processing parameters [6–8].

The primary effect of the part immersion depth has a small effect on Almen intensity, as shown in the Pareto chart in Fig. 6. However, the ANOVA in Table 5 shows that the two-factor interaction effects of immersion depth with eccentricity and frequency are as significant as the primary effects of eccentricity and frequency. This is observed in Fig. 10a and Fig. 10b by the smaller slopes for lower immersion depths (dashed lines) than for deeper part immersions (solid lines). This effect is attributed to the higher hydrostatic forces found deeper in the tub [21]. However, sufficient media kinetic energy is required for higher hydrostatic pressures. To better illustrate this effect, Fig. 11 shows the evolution of Almen intensity as a function of the immersion depth for different sets of eccentricity and frequency. For low eccentricity and frequency (blue solid line), increasing the immersion depth decreases the Almen intensity. When the penetration depth is maximum (28 cm), the Almen intensity is

irrelevant ( $-0.031$  mmN). This is because no media movement is observed at this depth for this low energy condition.

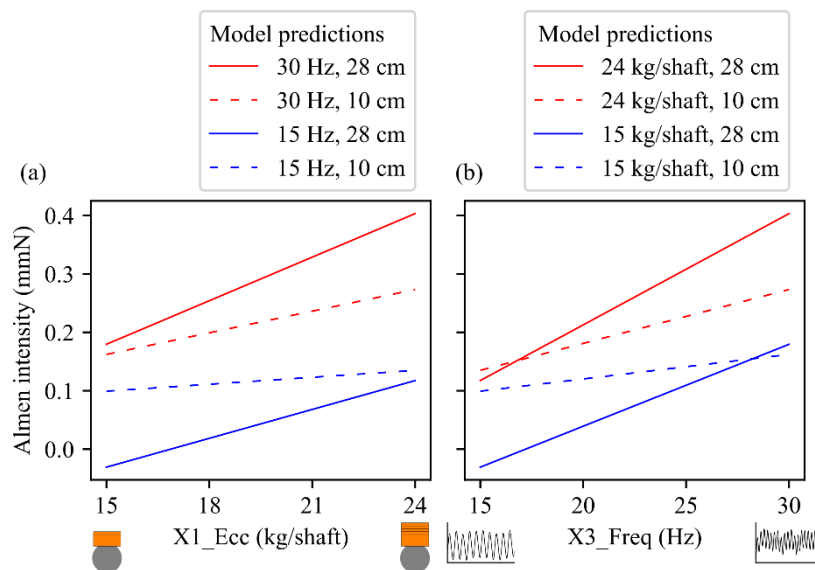


Fig. 10. Model profiler for the definitive empirical model. Almen intensities from Equation (7) are plotted as a function of (a) X1\_Ecc for the minimal and maximal values of X3\_Freq and X5\_Depth, (b) X3\_Freq for the minimal and maximal values of X1\_Ecc and X5\_Depth

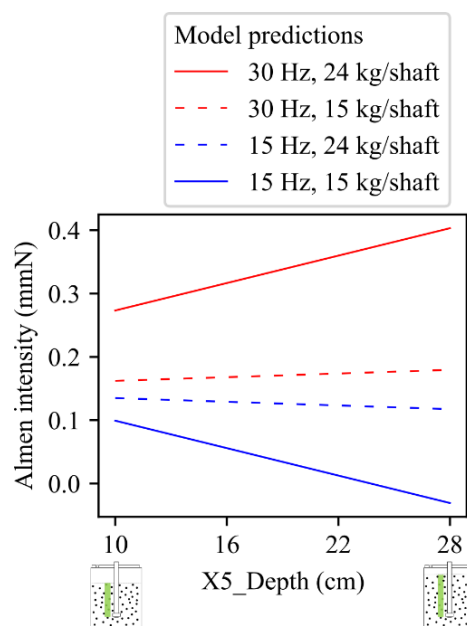


Fig. 11. Model profiler for the definitive empirical model. Almen intensities from Equation (7) are plotted as a function of (a) X5\_Depth for different tub energies, given by the levels of X1\_Ecc and X3\_Freq

On the contrary, for high eccentricity and frequency (red solid line), Almen intensity increases with the immersion depths. This suggests that a deeper tub is beneficial for the efficiency of the vibratory peening process provided the rotating shafts can supply sufficient energy to the media. For the set-up in this study, the highest Almen intensity of 0.198 mmA

(see Fig. 9) was achieved for 24 kg/shaft, 30 Hz and 28 cm. Canals et al. [6] reached a maximum Almen intensity of 0.25 mmA for a similar frequency (30 Hz). The difference can be attributed to higher eccentricity and immersion depth.

## 5. CONCLUSION

This work highlighted the effect of the vibratory peening process parameters on Almen intensity. A vibratory peening machine with a vertical tub movement and a flat bottom which rests on airbags was used. Seven process parameters were investigated within the same vibratory peening machine using the statistical tools from the design of experiments method.

The vibratory peening machine used in this study experimentally produced Almen intensities ranging from 0.084 mmN to 0.198 mmA. An empirical linear model was fitted to relate the effect of the three major vibratory peening parameters on Almen intensities. This model included primary effects and two-factors interactions of the statistically significant factors on Almen intensity. The linear variation of Almen intensity as a function of the frequency of the rotating shafts was confirmed except for one specific case. Further investigations are required on the vibration resonance modes of the tub, which could lead to different treatments.

The design of experiment method identified that the media mass in the tub, the airbags pressure, part longitudinal position and lubricant rate were minor factors. On the contrary, the rotating shaft eccentricity and frequency have the largest influence on Almen intensity. The specimen immersion depth is also of major importance on Almen intensity but only if the rotating shafts have sufficient eccentricity and frequency.

## REFERENCES

- [1] GANE D.H., RUMYANTSEV Y.S., DIEP H.T., BAKOW L., 2003, *Evaluation of Vibrostrengthening for Fatigue Enhancement of Titanium Structural Components on Commercial Aircraft*, Ti-2003 Science and Technology, Proceedings of the 10th World Conference on Titanium, Hamburg, Germany, 1053–8.
- [2] DELOSRIOS E.R., WALLEY A., MILAN M.T., HAMMERSLEY G., 1995, *Fatigue Crack Initiation and Propagation on Shot-Peened Surfaces in A316 Stainless Steel*, International Journal of Fatigue, 17, 493–499.
- [3] DOWLING N. E., 1998, *Mechanical Behavior of Materials*, ISBN-10 013905720X.
- [4] MEDIRATTA R., AHLUWALIA K., YEO S.H., 2016, *State-of-the-art on Vibratory Finishing in the Aviation Industry: An Industrial and Academic Perspective*, Int. J. Adv. Manuf. Technol., 85, 415–29.
- [5] FELDMANN G., WONG C.C., WEI W., HAUBOLD T., 2014, *Application of Vibropeening on Aero – Engine Component*, Procedia CIRP, 13, 423–428.
- [6] SANGID M.D., STORI J.A., FERRIERA P.M., 2011, *Process Characterization of Vibrostrengthening and Application to Fatigue Enhancement of Aluminum Aerospace Components–Part I, Experimental Study of Process Parameters*, Int. J. Adv. Manuf. Technol., 53, 545–60.
- [7] CANALS L., BADREDDINE J., MCGILLIVRAY B., MIAO H.Y., LEVESQUE M., 2019, *Effect of Vibratory Peening on the Sub-Surface Layer of Aerospace Materials Ti-6Al-4V and E-16NiCrMo13*, Journal of Materials Processing Technology, 264, 91–106.
- [8] CHAN W.L., AHLUWALIA K., GOPINATH A., 2019, *Parametric Study of Fixtured Vibropeening*, Metals, 9, 910.
- [9] GOPINATH A., CHAN W.L., KUMAR A.S., 2020, *Data Driven Optimization of Vibropeening*, Procedia CIRP, 87, 285–90.

- 
- [10] KUMAR D., IDAPALAPATI S., WANG W., 2021, *Influence of Residual Stress Distribution and Microstructural Characteristics on Fatigue Failure Mechanism in Ni-Based Superalloy*, *Fatigue Fract. Eng. Mat. Struct.*, 44, 1583–601.
- [11] ALCARAZ J.Y., ZHANG J., NAGALINGAM A.P., GOPASETTY S.K., TOH B.L., GOPINATH A., AHLUWALIA K., ANG M.G.W., YEO S.H., 2022, *Numerical Modeling of Residual Stresses During Vibratory Peening of a 3-Stage Blisk – a Multi-Scale Discrete Element and Finite Element Approach*, *Journal of Materials Processing Technology*, 299, 117383.
- [12] CAO W., FATHALLAH R., CASTEX L., 1995, *Correlation of Almen Arc Height with Residual Stresses in Shot Peening Process*, *Materials Science and Technology*, 11, 967–973.
- [13] MIAO H.Y., LAROSE S., PERRON C., LEVESQUE M., 2010, *An Analytical Approach to Relate Shot Peening Parameters to Almen Intensity*, *Surface Coatings Technology*, 205/7, 2055–2066.
- [14] SAE STANDARD J443, 2010, *Procedures for Using Standard Shot Peening Almen Strip*, [https://www.sae.org/standards/content/j443\\_201708/](https://www.sae.org/standards/content/j443_201708/).
- [15] KUMAR D., IDAPALAPATI S., WANG W., CHILD D.J., HAUBOLD T., WONG C.C., 2019, *Microstructure-Mechanical Property Correlation in Shot Peened and Vibro-Peened Ni-Based Superalloy*, *Journal of Materials Processing Technology*, 267, 215–229.
- [16] SAE STANDARD J442, 2009, *Test Strip, Holder, and Gage for Shot Peening*, <https://webstore.ansi.org/standards/sae/sae4422008j442>.
- [17] SAE STANDARD J2597, 2009, *Computer Generated Shot Peening Saturation Curves*, [https://www.sae.org/standards/content/j2597\\_201709/](https://www.sae.org/standards/content/j2597_201709/).
- [18] MONTGOMERY D. C., 2012, *Design and Analysis of Experiments*, Wiley.
- [19] SAE STANDARD AMS2430, 2015, *Shot Peening, Automatic*, <https://www.sae.org/standards/content/ams2430/>.
- [20] WANG S., TIMSIT R.S., SPELT J.K., 2000, *Experimental Investigation of Vibratory Finishing of Aluminum*, *Wear*, 243, 147–56.
- [21] HASHIMOTO F., JOHNSON S.P., CHAUDHARI R.G., 2016, *Modeling of Material Removal Mechanism in Vibratory Finishing Process*, *CIRP Annals*, 65, 325–328.